water

MDPI

Article

Determination of Optimal Water Intake Layer Using Deep Learning-Based Water Quality Monitoring and Prediction

Yunhwan Kim [1,†], Seoeun Kwak [2,†], Minhyeok Lee [1], Moon Jeong [1], Meeyoung Park [2,*] and Yong-Gyun Park [1,*]

[1] Department of Environmental and Energy Engineering, Chonnam National University, 77 Yongbong-ro, Buk-gu, Gwangju 61186, Republic of Korea; dbsghks288@gmail.com (Y.K.); xhdlr1215@naver.com (M.L.); munzeong@naver.com (M.J.)

[2] Department of Computer Engineering, Kyungnam University, 7 Gyeongnamdaehak-ro, Masanhappo-gu, Changwon-si 51767, Republic of Korea; act1793@student.kyungnam.ac.kr

* Correspondence: mpark@kyungnam.ac.kr (M.P.); ygpark7@jnu.ac.kr (Y.-G.P.); Tel.: +82-55-249-6491 (M.P.); +82-62-530-1856 (Y.-G.P.)

† These authors have contributed equally to this work.

Abstract: The effective management of drinking water sources is essential not only for maintaining their water quality but also for the efficient operation of drinking water treatment plants. A decline in water quality in water reservoirs can result in increased operational costs for water treatment and compromise the reliability and safety of treated water. In this study, a deep learning model, the long short-term memory (LSTM) algorithm, was employed to predict water quality and identify an optimal water intake layer across various seasons and years for Juam Lake, Korea. A comprehensive investigation was conducted to prioritize various water quality parameters and determine suitable intake layers. Based on these priorities, effective methods for optimizing an intake layer were developed to enable more reliable water intake operations. Water quality data from January 2013 to June 2023 were analyzed for the study. This dataset was used for rigorous statistical and correlational analyses to better understand the dynamics affecting water quality parameters. The findings aim to enhance the operational efficiency of water intake and treatment facilities.

Keywords: optimal intake layer; water treatment; drinking water source; water quality; deep learning model

check for updates

Citation: Kim, Y.; Kwak, S.; Lee, M.; Jeong, M.; Park, M.; Park, Y.-G. Determination of Optimal Water Intake Layer Using Deep Learning-Based Water Quality Monitoring and Prediction. *Water* **2024**, *16*, 15. https://doi.org/10.3390/w16010015

Academic Editor: Christos S. Akratos

Received: 14 November 2023
Revised: 14 December 2023
Accepted: 14 December 2023
Published: 20 December 2023

Copyright: © 2023 by the authors. Licensee MDPI, Basel, Switzerland. This article is an open access article distributed under the terms and conditions of the Creative Commons Attribution (CC BY) license (https://creativecommons.org/licenses/by/4.0/).

1. Introduction

Water is a critical resource used for various purposes, including human consumption, industrial processes, agriculture, and recreation [1]. However, declines in water resource quality, such as eutrophication and algal blooms, are increasingly common due to rapid urbanization, industrial growth, overpopulation, and climate change, all of which further harm aquatic habitats [2–4]. In Korea, a country with four distinct seasons, the quality of water sources is influenced by a variety of environmental factors. For example, due to seasonal variations, lakes and reservoirs typically experience vertical temperature gradients between the surface and deeper waters during summer and winter, causing thermal stratification [5]. In contrast, during spring and autumn, these temperature gradients diminish, resulting in vertical mixing in the water bodies [6].

Most large-scale water reservoirs encounter periods of thermal stratification, during which the water separates into distinct layers based on temperature [7]. This extended stratification impedes the reservoir's vertical mixing, leading to oxygen depletion in the lower layers and sediments, resulting in hypoxia [8,9]. It also releases ions such as iron, manganese, and phosphorus from the sediments into the water, causing aesthetic problems [6,8,10,11]. The issue of oxygen depletion in benthic ecosystems is closely related to algal blooms, which are considered a negative environmental consequence of eutrophication, mainly caused by excess nitrogen and phosphorus. Algal blooms not only lead

to oxygen depletion but also cause significant environmental and public health concerns such as odor and toxins [6,12–16]. For instance, the depletion of dissolved oxygen due to decaying algae can lead to mass mortality of benthic invertebrates. Additionally, the toxic effects of microcystin, a product related to algae, on living organisms are well-known from numerous studies [17,18]

Reservoirs are susceptible to water quality degradation, which can be caused by their hydrological properties, alterations in biogeochemical cycles, and various external environmental factors. Water contamination in reservoirs, which serve as sources of potable water, can cause multiple issues in the water treatment process, such as odor generation, filter media clogging, and so on. This can lead to increased water treatment costs and/or reduced reliability of the produced water [19].

Selective water intake involves adjusting the depth of water intake according to the water quality. This method is effective for on-site responses to deteriorating raw water quality [1,19]. To effectively address water quality issues through selective water intake, it is essential to understand the seasonal variations in water quality. This understanding enables water intake from layers with the best water quality. To comprehend the changes in the aquatic environment, various remote monitoring systems based on the Internet of Things (IoT) have been developed, leading to the collection of vast amounts of real-time data. Water quality prediction models can forecast water quality for specific future periods using both historical and real-time data collected by these remote water quality monitoring systems [20]. Recently, various advanced techniques, such as fuzzy mathematics, stochastic mathematics, 3S technology, and artificial neural networks (ANNs), have been introduced to enhance the applicability and reliability of water quality prediction models [21,22]. Among these, the long short-term memory (LSTM) model, a type of deep neural network, exhibits excellent performance in time-series predictions, resulting in its expanded use across various fields [23].

In this study, we used water quality data collected from Juam Lake through the national automatic water quality monitoring system from January 2013 to June 2023. The focus of our research was to investigate the optimal water intake layers using water quality predictions with a deep learning model. For this purpose, we employed the long short-term memory (LSTM) model, known for its excellent performance in recent time-series data analysis, to predict water quality. We applied the traditional LSTM algorithm rather than complex structured algorithms for rapid and accurate monitoring from IoT sensor data. Using this optimally trained model, we predicted the optimal intake layer for a one-year period. We thoroughly reviewed comprehensive water quality monitoring results to identify priorities among key water quality parameters for determining the most effective water intake layers. Ultimately, our study proposes a method for selecting the most suitable water intake layer based on our research findings.

2. Materials and Methods

2.1. Water Quality Standards

Korea does not have any legal provisions that explicitly mention standards for drinking water source quality. However, water quality standards included in the Enforcement Decree of The Framework Act on Environmental Policy can be regarded as standards for drinking water sources [24]. Table 1 shows the standards for lake water. The grades suitable for domestic water use are “Very good”, “Good”, “Slightly good”, and “Commonly”. The “Bad” and “Very bad” grades indicate water quality that, even if purified through water treatment processes, can only be used for industrial purposes. Specifically, if a lake is rated as “Very good”, it can be used for domestic purposes after relatively simple water treatments like filtration and disinfection. For “Good” and “Slightly good” grades, it can be used for domestic purposes after standard water treatments like filtration, sedimentation, and disinfection. On the other hand, for the “Commonly” grade, advanced water treatment processes, including filtration, sedimentation, activated carbon, and disinfection, are required to use the lake water for domestic purposes.

Table 1. Domestic Lake Water Quality Standards.

Standard / Grade	pH	COD (mg/L)	TOC (mg/L)	SS (mg/L)	DO (mg/L)	T-P (mg/L)	T-N (mg/L)	Chl-a (mg/m^3)	Total Coliforms	Fecal Coliforms
Very good (Ia)	6.5 to 8.5	≤2	≤2	≤1	≥7.5	≤0.01	≤0.2	≤5	≤50	≤10
Good (Ib)	6.5 to 8.5	≤3	≤3	≤5	≥5.0	≤0.02	≤0.3	≤9	≤500	≤100
Slightly good (II)	6.5 to 8.5	≤4	≤4	≤5	≥5.0	≤0.03	≤0.4	≤15	≤1000	≤200
Commonly (III)	6.5 to 8.5	≤5	≤5	≤15	≥5.0	≤0.05	≤0.6	≤20	≤5000	≤1000
Slightly bad (IV)	6.5 to 8.5	≤8	≤6	≤15	≥2.0	≤0.10	≤1.0	≤35	-	-
Bad (V)	6.5 to 8.5	≤10	≤8	Luggage, etc., is floating	≥2.0	≤0.15	≤1.5	≤70	-	-
Very bad (VI)	6.5 to 8.5	>10	> 8	-	<2.0	>0.15	>1.5	>70	-	-

Some water treatment plants in Korea implement a selective water intake when abnormal water quality is detected. This enables the selection of water from the layer with the most suitable quality by adjusting the intake depth. The water quality parameters used to determine abnormal conditions include algae, odor-causing substances, manganese, water temperature, pH, and turbidity. The criteria for abnormal water quality are based on the "Good" grade, which is a general requirement standard for drinking water source of a lake. Hence, if the water quality falls below the "Good" grade standards, adjustments to the intake layer are necessary.

Not all water quality parameters measured by the automatic monitoring network (AMN) are included in the source water quality standards. Specifically, the commonly applied parameters are dissolved oxygen (DO), total organic carbon (TOC), total nitrogen (T-N), total phosphorus (T-P), and pH, while standards for chlorophyll-a (Chl-a), electrical conductivity (EC), turbidity, and temperature are not specified. In Korea, Chl-a is used as a criterion for issuing algae alerts, and the advisory and alert thresholds for algae are set at 15 μg/L and 25 μg/L, respectively, based on two consecutive samples. In Australia's estuary management program, a Chl-a concentration of 20 μg/L is considered an indicator of potential algae occurrence [19]. For turbidity, the American Water Works Association recommends a level of 5 NTU or lower after the sedimentation phase in the water treatment process for the operation of sand filtration [25]. Thus, in this study, the thresholds for abnormal water quality for Chl-a and turbidity are set at 20 μg/L and 5 NTU, respectively, while EC and temperature have been excluded from the criteria for determining abnormal water quality.

2.2. Monitoring Sites of Juam Lake

The study area, Juam Lake, is an artificial lake constructed in 1991 in response to the increased water demand stemming from the development of large industrial complexes in Yeosu-si and Gwangyang-si, Korea, as well as the population growth in Gwangju-si. Currently, it provides both domestic and industrial water to cities including Gwangju, Suncheon, Gwangyang, and Yeosu [26]. The catchment area of Juam Lake is 1010 km^2, and its storage capacity is 457 million m^3 [27,28]. The study area with the locations of both automatic and manual monitoring stations is presented in Figure 1. Table 2 provides a summary of Juam Lake's specific hydrological features.

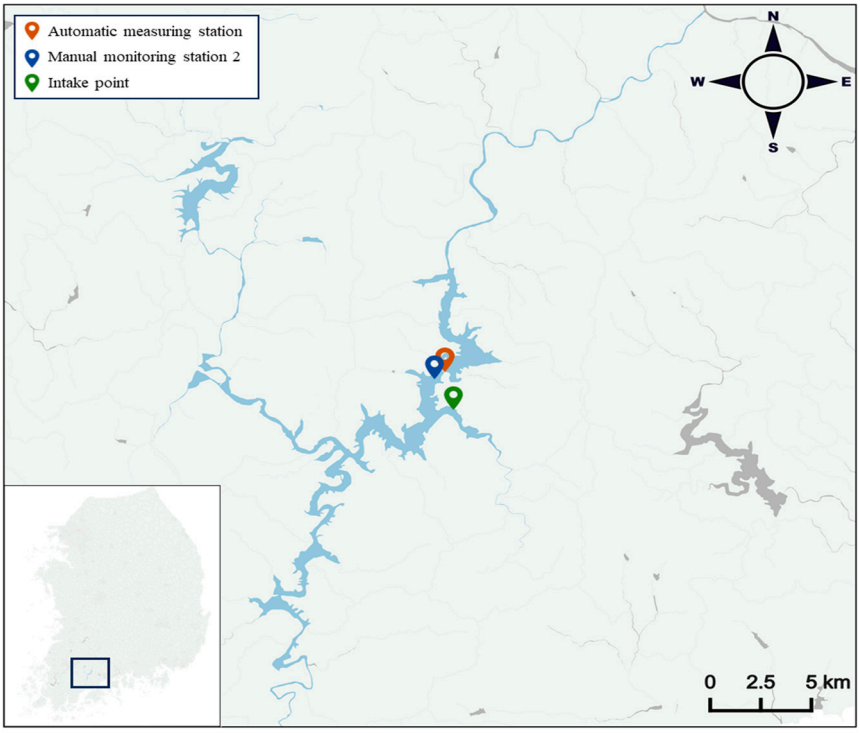

Figure 1. Automatic, manual water monitoring station and intake point in the study area.

Table 2. Hydrological characteristics of Lake Juam.

Category	Lake Juam
Surface area (km^2)	22
Water capacity ($\times 10^6$ m^3)	457
Average water volume ($\times 10^6$ m^3)	311
Annual water inflow ($\times 10^6$ m^3)	623
Annual water outflow ($\times 10^6$ m^3)	673
Maximum water level (m)	108.6
Average water level (m)	104.1
Drainage area (km^2)	1010

2.3. Long Short-Term Memory Model for Prediction

Long short-term memory (LSTM), a powerful deep learning algorithm, is characterized by its unique architecture, which includes memory cells and gate units [29–33]. It effectively resolves the vanishing gradient problem commonly encountered in recurrent neural networks (RNNs) [34] and, as a result, captures long-term dependencies. LSTM has successfully proven its effectiveness in various time-series sequence data processing tasks, such as signal analysis, natural language processing, and speech recognition [35–41]. On the other hand, classification algorithms such as XGBoost excel in classification problems, particularly in identifying class labels through multivariate analysis. Considering our objective to predict trends based on time-series data for a single parameter individually, we opted for LSTM over XGBoost due to its specialized capabilities in handling sequential data.

Basically, the LSTM architecture comprises a collection of interconnected sub-networks called memory blocks. The concept underlying these memory blocks is to preserve their state over time and control the information flow through non-linear gating units. Figure 2 illustrates the structure of a standard LSTM, encompassing gates, input signal x(t), output y(t), activation functions, and peephole connections [42]. The output is recurrently linked back to its input, including all the gates [32].

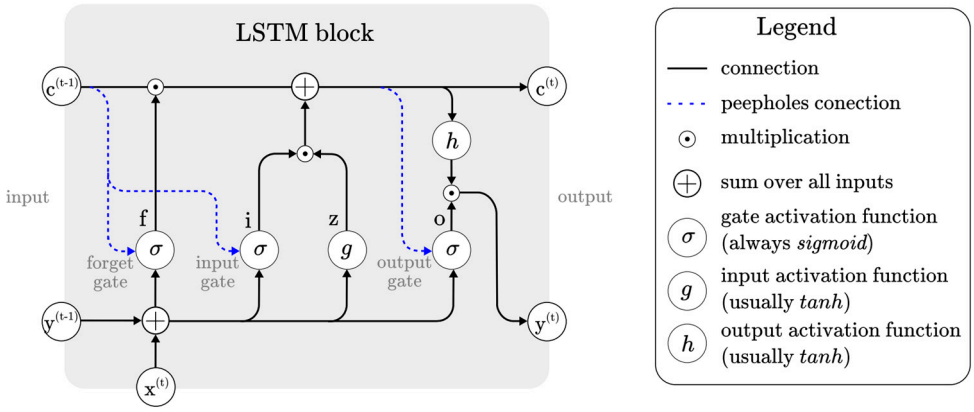

Figure 2. Architecture of a standard LSTM algorithm.

Recently, LSTM-based prediction models have been widely applied in water quality assessment research [20,43–47]. However, when using LSTM, there is a drawback in that for more accurate prediction results, the input values provided to LSTM must be accurate. Otherwise, it becomes challenging to have confidence in LSTM's prediction results. Therefore, in this study, we not only utilized LSTM but also conducted extensive data preprocessing to ensure the generation of accurate prediction values.

3. Results

3.1. Data Collection

The AMN, operational in major rivers and lakes in Korea, tracks water quality status and pollution levels in real-time, enabling prompt responses to pollution incidents. As of 2023, there are a total of 74 AMN stations installed nationwide. Common water quality parameters measured include temperature, DO, pH, EC, and TOC, along with 27 optional parameters like turbidity, Chl-a, and so on. The automatic water quality monitoring data are collected every hour. The water quality monitoring network (WQMN), unlike the AMN, requires manual measurements and is set up to understand the water quality status of major rivers, lakes, and other public water areas nationwide. The measured data also serve as foundational information for analyzing the effects of major water environmental policies as well as making new policies. For this study, water quality data were sourced from the AMN of Juam Lake. A comprehensive dataset consisting of 91,992 rows of water quality measurements was collected, including parameters such as temperature, pH, EC, DO, turbidity, TOC, T-N, T-P, and Chl-a, from 1 January 2013 to 30 June 2023.

Each water quality parameter can have different distributions depending on the water level due to the lake's hydrological characteristics and biogeochemical cycles. For the AMN, there is no variation in the measured water levels. However, with the WQMN data, since measurements are taken at the upper, middle, and lower layers, it is possible to discern the distribution characteristics of water quality parameters based on season and water level. Table 3 presents basic statistical analysis results for each water quality parameter, comparing automatic and manual monitoring data. The water quality for each parameter in the automatic monitoring data was most similar to the upper layer point in the manual water quality monitoring data. Moreover, in the manual monitoring data, the average temperature, pH, DO, TOC, and Chl-a decreased with increasing depth due to reduced light availability, microbial decomposition, chemical reactions, and so on. EC was lowest in the middle layer and highest in the lower layer. T-N was relatively high in the lower layer compared to that in the upper layer, while T-P remained consistent regardless of the water layer. In the automatic monitoring data, temperature, EC, and Chl-a showed relatively large standard deviations compared to those of other water quality parameters. Additionally, turbidity, T-P, and Chl-a exhibited relatively significant skewness. Particularly for turbidity, actual outliers were observed reaching very high values, resulting in a pronounced skewness in the data.

Table 3. Statistical analysis of water quality parameters by collected data.

	Automatic Monitoring Station						**Manual Measurement Point 2 (Upper Layer)**						**Manual Measurement Point 2 (Middle Layer)**						**Manual Measurement Point 2 (Lower Layer)**					
Parameters	**Avg.**	**Median**	**S.D.**	**Min**	**Max**	**Skewness**	**Avg.**	**Median**	**S.D.**	**Min**	**Max**	**Skewness**	**Avg.**	**Median**	**S.D.**	**Min**	**Max**	**Skewness**	**Avg.**	**Median**	**S.D.**	**Min**	**Max**	**Skewness**
Temp. (°C)	17.86	18.40	7.91	4.20	0.10	−0.084	16.71	17.90	8.12	1.00	32.00	−0.10	13.60	13.70	6.48	2.00	26.00	0.11	10.10	8.60	4.83	2.00	23.00	0.83
pH	7.57	7.40	0.75	6.30	10.00	0.63	7.81	7.80	0.69	6.30	9.80	0.39	7.20	7.20	0.65	4.80	8.30	−0.90	6.82	6.90	0.79	3.90	8.10	−0.87
EC (μs/cm)	80.30	79.00	10.87	54.00	127.00	0.47	81.86	81.50	9.70	59.00	107.00	−0.20	78.88	79.00	11.30	47.00	105.00	−0.14	85.94	82.50	15.67	59.00	156.00	1.45
DO (mg/L)	9.59	9.60	1.86	4.00	16.40	0.13	10.14	10.00	1.88	6.70	13.90	0.03	8.63	9.10	3.31	1.20	13.30	−0.50	7.32	7.95	3.93	0.10	13.10	−0.26
Turbidity (NTU)	1.77	1.40	1.94	0.10	138.90	19.05	-	-	-	-	-	-	-	-	-	-	-	-	-	-	-	-	-	-
TOC (mg/L)	1.68	1.60	0.28	0.10	3.90	0.62	1.81	1.80	0.29	1.20	2.50	0.37	1.71	1.70	0.21	1.30	2.50	0.50	1.62	1.60	0.23	1.10	2.50	0.66
T-N (mg/L)	0.66	0.64	0.21	0.10	1.75	0.68	0.73	0.71	0.21	0.40	1.72	1.85	0.84	0.75	0.32	0.42	2.35	2.24	0.83	0.76	0.24	0.45	1.81	1.78
T-P (mg/L)	0.01	0.01	0.004	0.003	0.07	2.20	0.02	0.01	0.01	0.01	0.04	1.44	0.02	0.01	0.01	0.003	0.06	2.05	0.02	0.01	0.01	0.002	0.05	1.41
Chl-a (mg/m^3)	8.90	6.90	8.28	0.10	134.00	4.14	6.15	5.40	4.35	0.30	21.80	1.28	5.13	4.80	4.15	0.20	26.90	2.12	3.34	2.70	2.58	0.10	12.70	0.92

3.2. Water Quality Characteristics of Juam Lake

The quality of drinking water sources can change due to their hydrological characteristics varying by season and external environmental parameters. Changes or deteriorations in the quality of water sources can directly or indirectly impact the subsequent water treatment processes, necessitating appropriate measures additionally. However, understanding the time-series characteristics and changes in water source quality is crucial because the magnitude of the impact and the corresponding processes differ for each water quality parameter during abnormal conditions. Figure 3 shows the trend of the collected automatic monitoring data and the abnormal water quality standards for each parameter. Figure 4 is a whisker box plot of the monthly variation in the collected monitoring data for the entire period. T-N was the parameter that most frequently fell below water quality standards, failing to meet them throughout most of the year regardless of the season. Subsequent to T-N, Chl-a exhibited numerous instances of water quality anomalies, primarily in the spring and summer seasons. Turbidity and pH showed consistent deviations from water quality standards, although to a lesser extent than T-N and Chl-a. Both turbidity and pH commonly exhibited abnormal standards, primarily in the summer. DO, TOC, and T-P generally satisfied water quality standards in most periods.

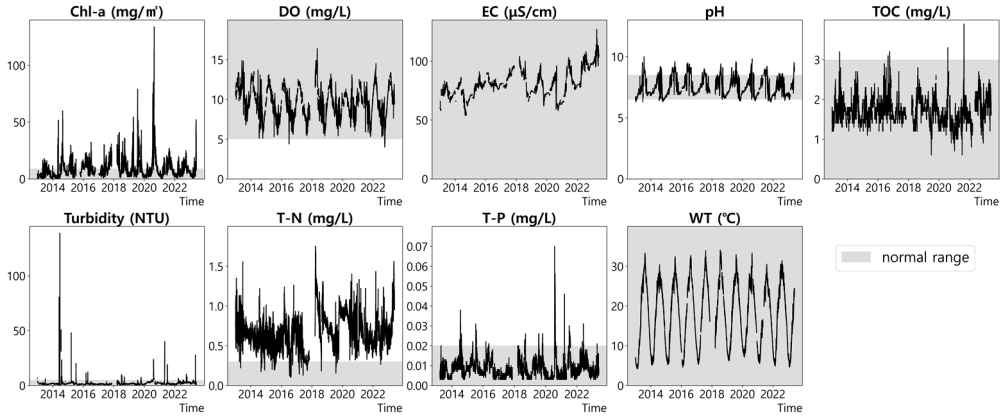

Figure 3. Raw data distribution of water quality parameters with a normal range (January 2013~December 2022).

The lake's mixing phenomenon brings nutrients from the deeper layers to the surface, enhancing algal blooms and eutrophication. Additionally, during the summer, the increased frequency of rainfall results in an influx of nutrients from external sources, exacerbating algal blooms and eutrophication. In this study, Chl-a, used as an indicator for algal blooms, along with T-P and TOC, showed an increasing trend in spring and summer. The frequency of outliers for these water quality parameters also increased. T-N showed a pattern of increasing in spring, decreasing in summer, and increasing again in autumn. Specifically, the monthly median values of TOC and T-P were highest in summer (1.9 mg/L and 0.01 mg/L, respectively), and Chl-a was highest in autumn with 12.4 mg/m^3. The median values of Chl-a, TOC, and T-P were lowest in winter (3.8 mg/m^3, 1.5 mg/L, and 0.006 mg/L, respectively). For T-N, the highest median value was 0.708 mg/L in spring, and the lowest was 0.562 mg/L in summer. Furthermore, algal growth depletes the DO in the lake, so DO showed a trend opposite to that of Chl-a, TOC, and T-P. It was observed that DO increased from the cold winter season, peaked in the spring, and then decreased until autumn. The highest median value of DO occurred in spring at 11.8 mg/L, and the lowest was in the autumn at 7.4 mg/L. Finally, turbidity generally showed a similar trend throughout the seasons, but a notably higher frequency of anomalies was observed in summer when rainfall was concentrated.

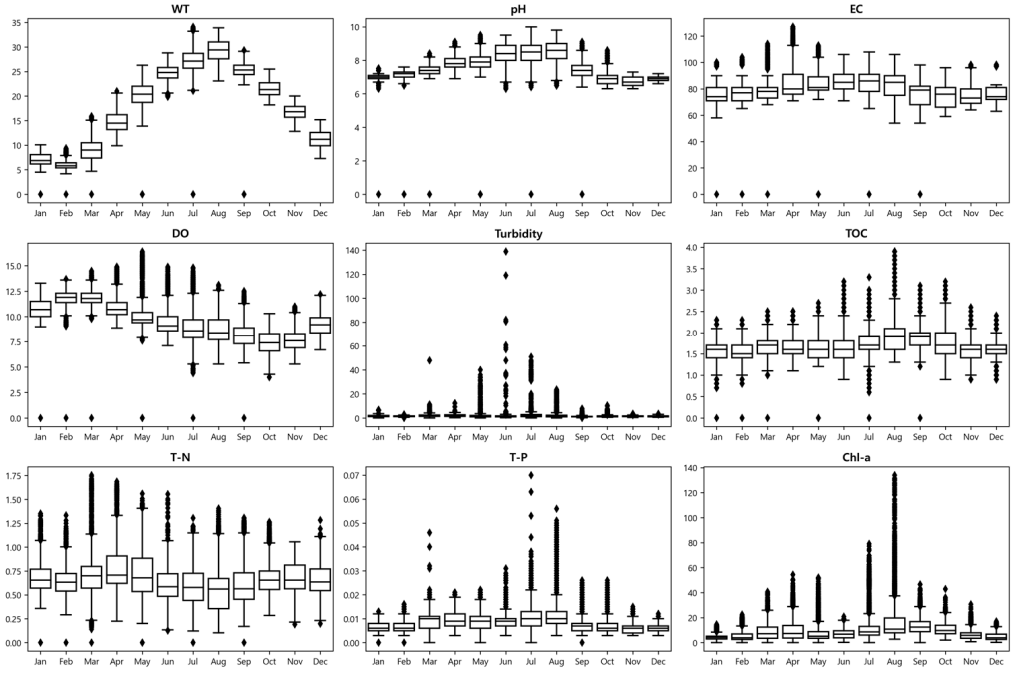

Figure 4. Monthly variation in collected data for water quality parameters.

3.3. Correlation of Water Quality Parameters

A correlation analysis was conducted based on the collected data to determine whether the water quality parameters were related to each other. Figure 5 shows the Pearson correlation coefficients between the parameters. Firstly, DO and pH have a weak negative linear relationship. As pH decreases, the increased H^+ ions react with the oxygen in the water, resulting in a decrease in DO. Therefore, simply by the chemical equilibrium between pH and DO, pH can generally have a positive linear relationship with DO [48]. However, this relationship can be altered by a combination of factors such as algal photosynthesis, aquatic respiration, water temperature, and the oxidative decomposition of organic matter, which may result in an opposite correlation trend [48]. DO also showed a moderate negative linear relationship with water temperature, with the lowest values in autumn and a steady increase until early spring. During the rainy season, large amounts of non-point sources of pollution near the lake can enter the lake, and DO can be consumed to break them down [49]. Therefore, water temperature and DO can form a non-linear relationship due to the seasonal nature of the rainy season that forms during the summer [49].

Meanwhile, Chl-a showed a positive linear relationship with turbidity, TOC, T-N, and T-P and a moderate positive linear relationship with pH ($0.3 < r \leq 0.7$). pH is closely related to algae. During photosynthesis, algae rapidly convert CO_2 in water to HCO_3^-. The HCO_3^- produced during this process dissociates back into OH^- and CO_2, which ultimately raises the pH of the water. Therefore, given the general relationship between pH and algae, there may be a positive linear relationship between Chl-a, an indirect indicator of algae, and pH [48]. In addition, T-P and turbidity, water temperature and turbidity, and water temperature and pH demonstrate moderate positive linear relationships. T-N and T-P, which cause eutrophication, are proportional to the load of organic pollutants, and Chl-a linearly increases with the rise in concentrations of T-N and T-P [50]. Therefore, as pollutants such as agricultural, industrial, and domestic effluents enter the water, T-N, T-P, and TOC concentrations increase while DO concentrations decrease [51].

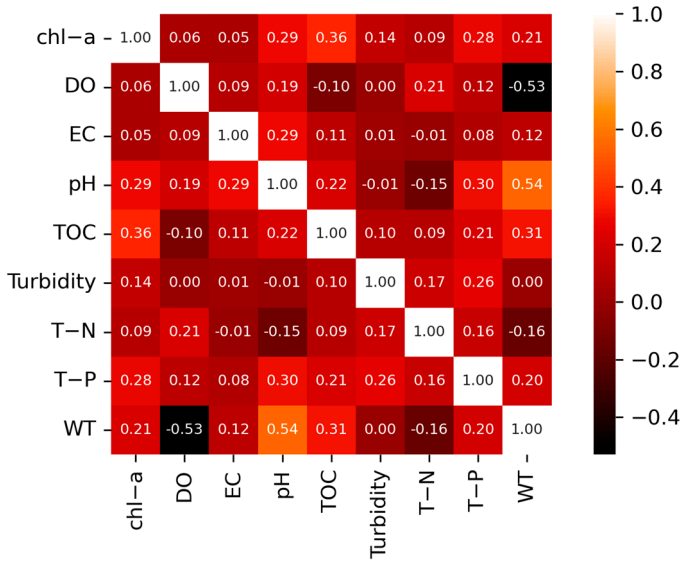

Figure 5. Correlation analysis between water quality parameters.

3.4. Data Preprocessing

Water quality data typically show continuity and change gradually and steadily [44]. Occasionally, due to equipment malfunctions or incorrectly collected data within the system, outliers can be recorded, exceeding the normal range, and missing values can also be present. Given the characteristics of water quality data, distinguishing whether an outlier is an error can be challenging, as short-term spikes in data may occur due to non-point source pollution or chance events, such as extreme rainfall [52].

In this study, we defined the normal range of the data to be within the interquartile range (IQR), precisely between the lower inner fence (LIF) at Q1 − 1.5 × IQR and the upper inner fence (UIF) at Q3 + 1.5 × IQR. The distribution of data within this normal range for each water quality parameter was visualized using box plots, along with outliers. Outlying data points were replaced with the minimum or maximum values within the normal range. The final adjusted data distributions are shown in Figure 6.

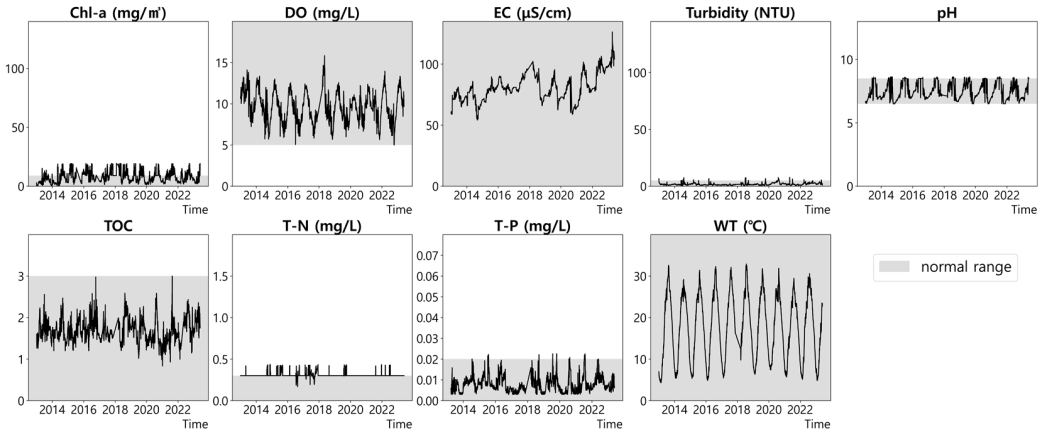

Figure 6. Adjusted data distribution for water parameters (January 2013~December 2022).

For addressing missing values, a statistical imputation method such as interpolation was applied. Preprocessing for missing data by filling with a single value like the mean or median carries the risk of replacing actual values with different ones. To maintain the trend of the original data and minimize loss, we employed interpolation. However, for cases where consecutive missing values occurred in a sequence of three or fewer, we filled them with the preceding value.

3.5. LSTM Model Training and Performance Evaluation

The LSTM deep learning model consisted of two LSTM layers and an output layer. Each LSTM layer had 50 nodes, and the hyperbolic tangent (tanh) activation function was used. Prior to model training, to prevent overfitting and evaluate the performance of the model, we split the entire dataset into training and test sets in a 7:3 ratio. Additionally, to improve the convergence speed of the models and reduce training time, the Min–Max normalization scaling technique was applied.

We trained the model by adjusting hyperparameters. We found the best model parameters by tuning the most critical hyperparameters in LSTM, including the time steps, prediction period, epochs, and batch size. The time step, representing the sequence of input data, was set to 168 h, while the prediction period, representing the sequence of output data, was set to 24 h, encompassing 7 days of observation and 1 day of prediction. We compared epochs at 200, 300, 500, and 700 and batch sizes of 32 and 64, respectively.

Subsequently, we conducted model performance evaluation. The evaluation was performed using the RMSE (root mean squared error), and we visualized the predicted results of the trained model based on the hyperparameters, such as epochs and batch sizes, through time-series graphs (Figure 7). Table 4 shows the optimal LSTM models along with their corresponding epochs and batch sizes for each water quality parameter.

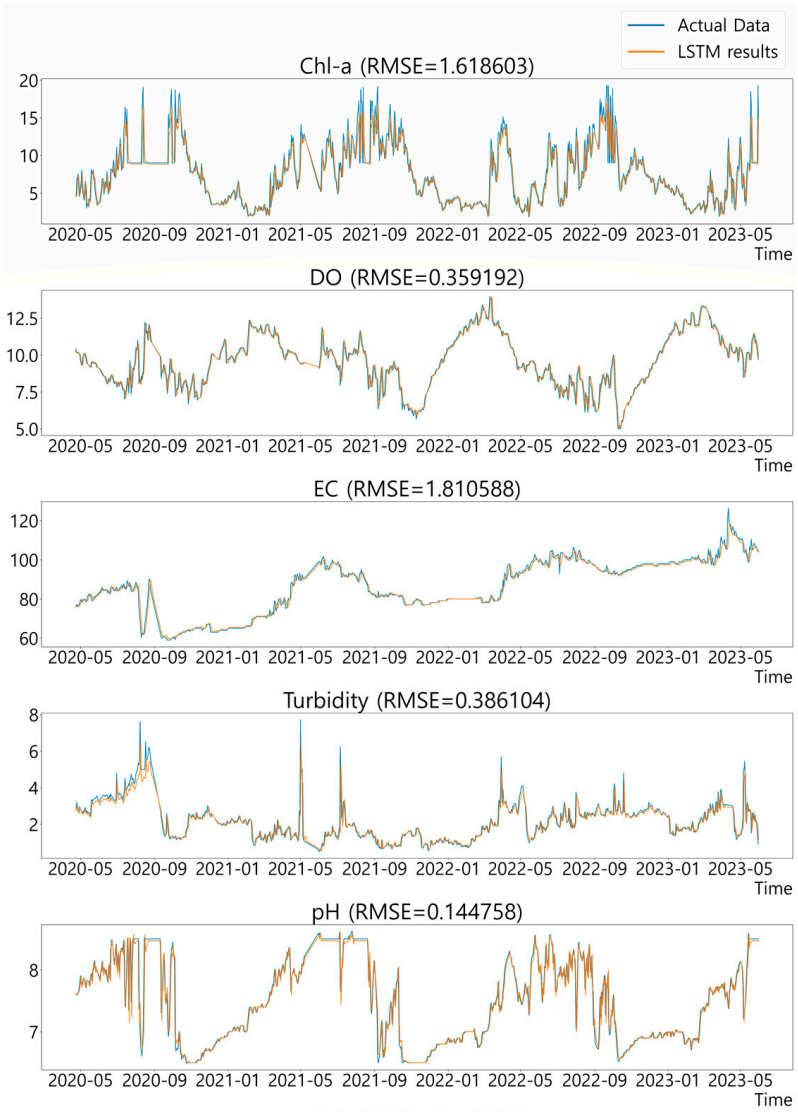

Figure 7. *Cont.*

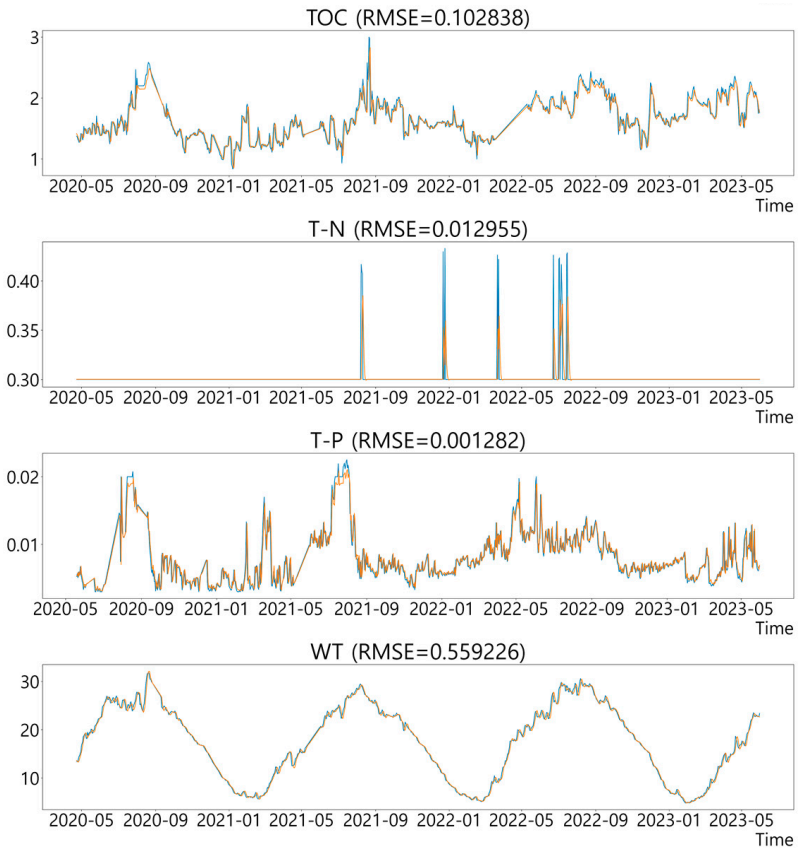

Figure 7. The performance of optimal LSTM model.

Table 4. The RMSE results of the optimal LSTM model for each parameter.

	Chl-a	DO	EC	Turbidity	pH	TOC	T-N	T-P	WT
Epoch	700	700	700	700	700	700	700	700	700
Batch size	32	32	32	32	32	32	32	32	32
RMSE	1.619	0.359	1.811	0.386	0.145	0.103	0.013	0.001	0.559

3.6. Prioritizing Water Quality Factors Based on Water Treatment Difficulty

Changes and degradation in the quality of the source water can impact the operational methods and conditions of drinking water treatment plants, often involving a diverse array of complex factors. This study identified and prioritized the challenges associated with various water quality factors in the water treatment process. These prioritization levels were used to determine the most suitable water intake layer in cases of complex water quality changes. The findings are summarized in Table 5.

Table 5. Water treatment difficulty by water quality factor.

Depth Selection Metrics	Chl-a	TOC	T-N	T-P	Turbidity	pH	DO	WT	EC
Relative difficulty of water purification	1	2	2	2	3	4	5	5	-

The effectiveness of water treatment methods against algae varies based on the specific species. Specifically, blue-green algae produce by-products like odor-causing substances such as 2-MIB and geosmin, as well as toxic compounds like microcystin-LR. Diatoms lead to filtration issues due to species like Synedra and Aulacoseira. In addition, blue-green algae, diatoms, and green algae all cause water turbidity issues [53]. Geosmin, 2-MIB, and microcystin-LR can be categorized as either soluble or particulate based on their form.

Particulate compounds can be eliminated through standard water treatment processes like flocculation, sedimentation, and filtration. In contrast, soluble compounds can primarily be removed using powdered activated carbon (PAC). Enhancing treatment efficiency can be achieved by employing ozone or dichlorination [54]. Precise care is essential when handling blue-green algae. Preliminary chlorination can break up these algae colonies, causing cells to scatter and seep into the filtrate. Therefore, it is crucial first to reduce their presence through flocculation and sedimentation. Following that, intermediate chlorination can help minimize the production of THMs and odors.

Particulate solids causing turbidity can be divided into organic and inorganic substances. Organic particles from algae, including green algae, can be almost 100% removed through standard solid-matter water treatment processes [55]. Non-algal particulate solids that flow into water during rainfall or stratification and are then collected and are also mostly removed through standard water treatment processes designed for solid removal [56]. As for pH, it can be adjusted using pH-adjusting agents such as H_2SO_4 and CO_2. Typically, iron and aluminum coagulants dissolve in water as acidic salts, reducing the pH. Thus, depending on the alkalinity and pH of the raw water, lime or alkali materials should be added to counteract the pH decrease. For aluminum sulfate ($Al_2(SO_4)_3$), the optimal pH for coagulation is between 6 and 7. Iron-based coagulants have a wider pH range of 5 to 11, broader than that of the aluminum type [57]. However, since the oxidation process of the iron component is essential for the coagulation process in iron-based coagulants, pH adjustment is necessary regardless of the type of coagulant used [58].

Algae requiring additional processes beyond chemical treatment were considered the most challenging, and Chl-a was given the highest priority for selective withdrawal because it is used as an indirect indicator of algal blooms. TOC, T-N, and T-P are used as indirect indicators of eutrophication and were given the highest priority after Chl-a due to the close correlation between eutrophication and algal blooms. The next priority was given to turbidity, which requires flocculation treatment processes, and pH, which requires additional chemical treatment, was considered the next priority after turbidity. Water temperature and DO were given the lowest priority due to their relatively low direct impact on the water treatment process.

3.7. Selection of the Optimal Intake Layer Based on Water Quality Factors

When the quality of the intake water source is deteriorated, it is crucial to draw water from the depth that has the highest water quality. Doing this minimizes water purification costs and enhances the safety of drinking water [19]. For this study, we have categorized the water supply into three layers: lower, middle, and upper. We then identified the best layer for water intake by examining and comparing the different water quality parameters and their respective challenges in water treatment, as presented in Table 6.

Table 6. Appropriate water intake layer by water quality factor.

Depth Selection Metrics	Chl-a	TOC	T-N	T-P	Turbidity	pH	DO	WT	EC
Relative difficulty of water purification	Middle layer	Upper layer	Upper layer	Upper layer	Upper layer	Middle layer	Upper layer	Upper layer	-

When algal blooms occur in Korea, it is necessary for operators to draw water from below the depth where the algae are growing, as the concentration of algae decreases with greater depth. Despite this, drawing water from the very bottom layer is not advisable due to high levels of iron and manganese in the sediments. Consequently, if the Chl-a levels in the upper layer do not meet the water quality standards, the middle layer is chosen as the water intake layer. Additionally, eutrophication, which is an excess of nutrients in water, encourages the growth of algae. As a result, when TOC, T-N, and T-P, which are indirect indicators of eutrophication, go beyond acceptable water quality levels, we need to take water from the middle or lower layers where there are typically fewer algae.

Turbidity, caused by rainfall or movement within the water column, might initially be the same throughout all layers. However, it eventually settles from the upper layers down to the lower layers due to gravity over time [59]. So, during times when there are fewer algae, if the turbidity surpasses the acceptable levels, we choose to draw water from the upper layer. This is because turbidity tends to be relatively low in the upper water layer. Moreover, as Table 3 presents, pH and DO levels usually decrease as water becomes deeper. They are generally higher in the euphotic zone, which gets plenty of sunlight, than in the aphotic zone, where there is a lack of sunlight [60].

Turbidity from rainfall or water column conduction may be similar across all layers depending on water depth but is transferred from upper to lower layers by gravitational settling over time [59]. Therefore, if turbidity exceeded the criteria during the algae-free period, the upper water layer was selected because the turbidity was relatively low in the upper water layer. Furthermore, as shown in Table 2, pH and DO levels tend to decrease with increasing water depth. They are typically higher in the euphotic zone, where sunlight is abundant, than in the aphotic zone, where sunlight is scarce [60]. Regarding pH, there is a specific range that works best with the type of flocculant used in treating water. Consequently, we chose to draw water from the middle layer, as it has pH values in a moderate range, avoiding the extreme highs or lows that can be found in the upper and lower layers. If the pH is outside the acceptable range, it could cause problems. When it comes to dissolved oxygen (DO), higher levels are preferable, leading us to opt for water from the upper layer if the DO falls below the standard. Lastly, while water temperature does not directly indicate pollution, it can influence standard water treatment processes like flocculation and sedimentation. In particular, cooler water temperatures can increase the water's viscosity, making it harder for flocs to form and for coagulants to be transported, which can hinder the treatment process [61].

3.8. Selection of the Optimal Water Intake Layer Based on Water Quality Prediction

The quality of water at its source is influenced by various hydrological, biological, and environmental factors, and it also exhibits seasonal variations. By predicting these seasonal changes in water quality and determining the corresponding optimal intake layer, operators can make more informed decisions and run water treatment plants more effectively. In this section, we introduce a mechanism for selecting the intake layer, which has been developed considering the previously established priorities and suitable intake layers for each water quality factor. Additionally, we provide an analysis of the annual optimal intake layer for Juam Lake, utilizing predicted data.

The comprehensive decision process for determining the optimal water intake layer is outlined as follows: (1) We prepared an input dataset consisting of 10 years of water quality measurements, including parameters such as temperature, pH, EC, DO, turbidity, TOC, T-N, T-P, and Chl-a. (2) An LSTM model was trained for each parameter using this 10-year dataset. (3) Next, the most effectively trained LSTM model for each parameter was selected. (4) Using these models, we predicted the future trends of each parameter, focusing on the changes in values. (5) These predictions were then used to identify the most suitable lake layer for water intake based on the predicted trends.

As shown in Figure 8, we determined whether the water source was contaminated by following a set order of priority for each water quality factor. If a specific water quality factor indicated contamination, we then selected the most suitable intake layer to minimize its impact on the water treatment process. By transforming the predicted water quality data into weekly average values, we were able to analyze how the recommended intake layer varied week by week. Withdrawals from the upper layer were most common, occurring for the majority of weeks, followed by withdrawals from the middle layer. The key water quality factor influencing middle layer intake was Chl-a. On the other hand, T-N was the main factor for upper layer intake. Throughout the year, water was drawn from the middle layer for a total of 17 weeks, mainly in early spring and summer. The upper layer was selected for the remaining 35 weeks due to T-N levels exceeding water quality standards.

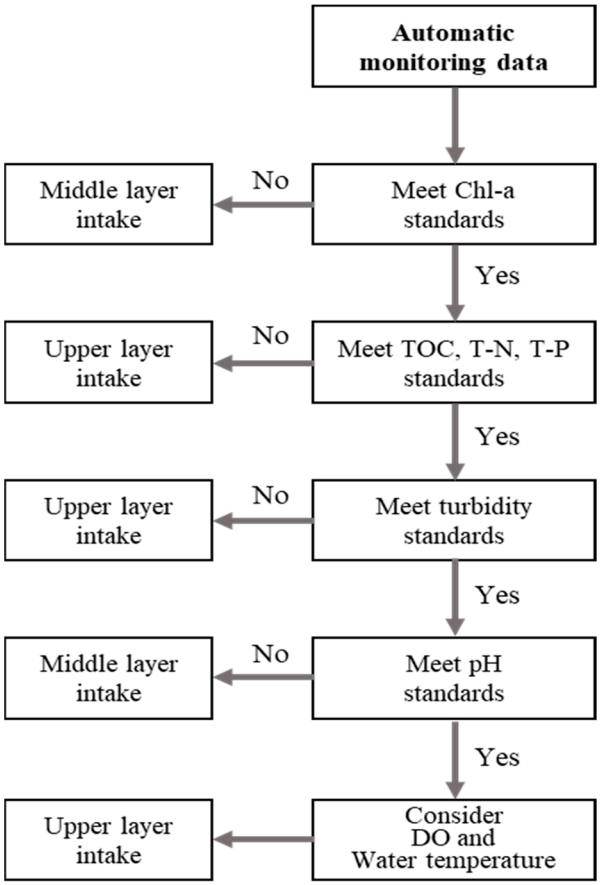

Figure 8. The process for the selection of the source water intake layer.

4. Conclusions

Effective management of water sources is essential for operating drinking water treatment plants efficiently and providing safe drinking water to consumers. Therefore, continuously monitoring the quality of water sources and effectively predicting changes in water quality can greatly affect the operational efficiency of water treatment plants and the quality of the water they produce. In this study, we investigated the seasonal variations in the water quality of Juam Lake and explored the interrelationships among water quality parameters using statistical and correlational analyses. Furthermore, we conducted predictions of water quality changes with an LSTM using 10 years of automated water quality monitoring data and proposed an optimal water intake layer. An in-depth investigation was undertaken to devise a strategy for choosing the optimal intake layer based on the predicted water quality.

Our investigation revealed that T-N was the water quality factor that contributed most significantly to the deterioration of water quality, followed by chlorophyll-a. Seasonally, the pH tended to increase in the summer due to algal blooms, with EC rising accordingly. In the spring, chlorophyll-a, TOC, T-P, and T-N levels tended to increase as nutrients were relatively abundant. DO levels were highest in spring and then decreased in autumn. Lastly, a very high frequency of turbidity outliers was observed during the summer, coinciding with the period of concentrated annual precipitation.

Applying a mechanism to choose optimal water intake layers based on water quality predictions with the LSTM model, the top layer, affected by T-N, was selected most often for 35 weeks in a year. The middle layer was chosen for 17 weeks during early spring and summer, influenced by Chl-a. In conclusion, our results will contribute to improving the operational efficiency of water intake and treatment facilities by accurately and promptly monitoring their performance.

Author Contributions: Conceptualization, M.P. and Y.-G.P.; Investigation, Y.K., S.K., M.L. and M.J.; Writing—original draft, Y.K. and S.K.; Writing—review & editing, M.P. and Y.-G.P.; Supervision, M.P. and Y.-G.P. All authors have read and agreed to the published version of the manuscript.

Funding: This work was supported by the Korea Ministry of Environment (Project for Development of Disaster Response Technology for Environmental Facilities, Project No.: 2022002860001) and the National Research Foundation of Korea (NRF) grant funded by the Korea government (MSIT) (No. RS-2023-00252141).

Data Availability Statement: Data is contained within the article.

Conflicts of Interest: The authors declare no conflict of interest.

References

1. Saadatpour, M.; Javaheri, S.; Afshar, A.; Solis, S.S. Optimization of selective withdrawal systems in hydropower reservoir considering water quality and quantity aspects. *Expert Syst. Appl.* **2021**, *184*, 115474. [CrossRef]
2. Ly, Q.V.; Lee, M.-H.; Hur, J. Using fluorescence surrogates to track algogenic dissolved organic matter (AOM) during growth and coagulation/flocculation processes of green algae. *J. Environ. Sci.* **2019**, *79*, 311–320. [CrossRef]
3. Xia, R.; Zhang, Y.; Wang, G.; Zhang, Y.; Dou, M.; Hou, X.; Qiao, Y.; Wang, Q.; Yang, Z. Multi-factor identification and modelling analyses for managing large river algal blooms. *Environ. Pollut.* **2019**, *254*, 113056. [CrossRef]
4. Song, K.; Fang, C.; Jacinthe, P.-A.; Wen, Z.; Liu, G.; Xu, X.; Shang, Y.; Lyu, L. Climatic versus anthropogenic controls of decadal trends (1983–2017) in algal blooms in lakes and reservoirs across China. *Environ. Sci. Technol.* **2021**, *55*, 2929–2938. [CrossRef]
5. Wetzel, R.G.; Limnology, G. Lake and river ecosystems. *Limnology* **2001**, *37*, 490–525.
6. Lee, Y.G.; Kang, J.-H.; Ki, S.J.; Cha, S.M.; Cho, K.H.; Lee, Y.S.; Park, Y.; Lee, S.W.; Kim, J.H. Factors dominating stratification cycle and seasonal water quality variation in a Korean estuarine reservoir. *J. Environ. Monit.* **2010**, *12*, 1072–1081. [CrossRef]
7. Lu, Y.; Tuo, Y.; Xia, H.; Zhang, L.; Chen, M.; Li, J. Prediction model of the outflow temperature from stratified reservoir regulated by stratified water intake facility based on machine learning algorithm. *Ecol. Indic.* **2023**, *154*, 110560. [CrossRef]
8. Hamilton-Taylor, J.; Smith, E.; Davison, W.; Sugiyama, M. Resolving and modeling the effects of Fe and Mn redox cycling on trace metal behavior in a seasonally anoxic lake. *Geochim. Cosmochim. Acta* **2005**, *69*, 1947–1960. [CrossRef]
9. Dai, M.; Guo, X.; Zhai, W.; Yuan, L.; Wang, B.; Wang, L.; Cai, P.; Tang, T.; Cai, W.-J. Oxygen depletion in the upper reach of the Pearl River estuary during a winter drought. *Mar. Chem.* **2006**, *102*, 159–169. [CrossRef]
10. Lamping, J.; Worrall, F.; Morgan, H.; Taylor, S. Effectiveness of aeration and mixing in the remediation of a saline stratified river. *Environ. Sci. Technol.* **2005**, *39*, 7269–7278. [CrossRef]
11. Tobiason, J.E.; Bazilio, A.; Goodwill, J.; Mai, X.; Nguyen, C. Manganese removal from drinking water sources. *Curr. Pollut. Rep.* **2016**, *2*, 168–177. [CrossRef]
12. Ly, Q.V.; Nguyen, X.C.; Lê, N.C.; Truong, T.-D.; Hoang, T.-H.T.; Park, T.J.; Maqbool, T.; Pyo, J.; Cho, K.H.; Lee, K.-S. Application of Machine Learning for eutrophication analysis and algal bloom prediction in an urban river: A 10-year study of the Han River, South Korea. *Sci. Total Environ.* **2021**, *797*, 149040. [CrossRef] [PubMed]
13. Jarvie, H.P.; Smith, D.R.; Norton, L.R.; Edwards, F.K.; Bowes, M.J.; King, S.M.; Scarlett, P.; Davies, S.; Dils, R.M.; Bachiller-Jareno, N. Phosphorus and nitrogen limitation and impairment of headwater streams relative to rivers in Great Britain: A national perspective on eutrophication. *Sci. Total Environ.* **2018**, *621*, 849–862. [CrossRef] [PubMed]
14. Huisman, J.; Codd, G.A.; Paerl, H.W.; Ibelings, B.W.; Verspagen, J.M.; Visser, P.M. Cyanobacterial blooms. *Nat. Rev. Microbiol.* **2018**, *16*, 471–483. [CrossRef] [PubMed]
15. Ly, Q.V.; Maqbool, T.; Hur, J. Unique characteristics of algal dissolved organic matter and their association with membrane fouling behavior: A review. *Environ. Sci. Pollut. Res.* **2017**, *24*, 11192–11205. [CrossRef] [PubMed]
16. Xin, X.; Zhang, H.; Lei, P.; Tang, W.; Yin, W.; Li, J.; Zhong, H.; Li, K. Algal blooms in the middle and lower Han River: Characteristics, early warning and prevention. *Sci. Total Environ.* **2020**, *706*, 135293. [CrossRef]
17. Li, X.; Li, J.; Meng, F.; Yao, L. Hepatotoxicity and immunotoxicity of MC-LR on silver carp. *Ecotoxicol. Environ. Saf.* **2019**, *169*, 28–32. [CrossRef] [PubMed]
18. Chen, L.; Giesy, J.P.; Xie, P. The dose makes the poison. *Sci. Total Environ.* **2018**, *621*, 649–653. [CrossRef]
19. Yang, W.-M. *Development of Rule-Based Operation Method for Selecting Optimal Water Quality when Taking Raw Water from Lakes*; Chonnam National University: Gwangju, China, 2023.
20. Liu, P.; Wang, J.; Sangaiah, A.K.; Xie, Y.; Yin, X. Analysis and prediction of water quality using LSTM deep neural networks in IoT environment. *Sustainability* **2019**, *11*, 2058. [CrossRef]
21. Maier, H.R.; Jain, A.; Dandy, G.C.; Sudheer, K.P. Methods used for the development of neural networks for the prediction of water resource variables in river systems: Current status and future directions. *Environ. Model. Softw.* **2010**, *25*, 891–909. [CrossRef]
22. Lee, S.; Lee, D. Improved prediction of harmful algal blooms in four Major South Korea's Rivers using deep learning models. *Int. J. Environ. Res. Public Health* **2018**, *15*, 1322. [CrossRef] [PubMed]
23. Huang, C.-J.; Kuo, P.-H. A deep CNN-LSTM model for particulate matter (PM2.5) forecasting in smart cities. *Sensors* **2018**, *18*, 2220. [CrossRef] [PubMed]

24. Kim, D.-W. Differences in Quality Standards between Reservoir Water and Tap Water. 2014. Available online: https://www.waterjournal.co.kr/news/articleView.html?idxno=21917 (accessed on 2 December 2014).
25. Moreira, V.R.; Guimarães, R.N.; Moser, P.B.; Santos, L.V.; de Paula, E.C.; Lebron, Y.A.; Silva, A.F.R.; Casella, G.S.; Amaral, M.C. Restrictions in water treatment by conventional processes (coagulation, flocculation, and sand-filtration) following scenarios of dam failure. *J. Water Process Eng.* **2023**, *51*, 103450. [CrossRef]
26. Lee, H.-N.; Jung, K.-S.; Cheon, G.-H.; Hur, Y.-T. A Investigation and Analysis of Water Temperature by Juam Regulation Dam Outflow in Downstream and Suncheon Bay. *Korea Water Resour. Assoc.* **2015**, *48*, 501–509. [CrossRef]
27. Lee, G.-S.; Kim, T.-K. Estimation of Nonpoint Source Pollutant Loads of Juam-Dam Basin Based on the Classification of Satellite Imagery. *Korean Assoc. Geogr. Inf. Studi* **2012**, *15*, 1–12.
28. Kim, B.-C.; Park, J.-H.; Heo, W.-M.; Lim, B.-J.; Hwang, G.-S.; Choi, K.-S.; Choi, J.-S. The Limnological Survey of Major Lakes in Korea (4): Lake Juam. *Korean J. Limnol.* **2001**, *18*, 81–95.
29. Hochreiter, S.; Schmidhuber, J. Long short-term memory. *Neural Comput.* **1997**, *9*, 1735–1780. [CrossRef] [PubMed]
30. Graves, A. Long short-term memory. In *Supervised Sequence Labelling with Recurrent Neural Networks*; Springer: Berlin/Heidelberg, Germany, 2012; pp. 37–45.
31. Staudemeyer, R.C.; Morris, E.R. Understanding LSTM—A tutorial into long short-term memory recurrent neural networks. *arXiv* **2019**, arXiv:1909.09586.
32. Yu, Y.; Si, X.; Hu, C.; Zhang, J. A review of recurrent neural networks: LSTM cells and network architectures. *Neural Comput.* **2019**, *31*, 1235–1270. [CrossRef]
33. Van Houdt, G.; Mosquera, C.; Nápoles, G. A review on the long short-term memory model. *Artif. Intell. Rev.* **2020**, *53*, 5929–5955. [CrossRef]
34. Graves, A.; Fernández, S.; Gomez, F.; Schmidhuber, J. Connectionist temporal classification: Labelling unsegmented sequence data with recurrent neural networks. In Proceedings of the 23rd International Conference on Machine Learning, New York, NY, USA, 25–29 June 2006; pp. 369–376.
35. Soutner, D.; Müller, L. Application of LSTM neural networks in language modelling. In Proceedings of the Text, Speech, and Dialogue: 16th International Conference, TSD 2013, Pilsen, Czech Republic, 1–5 September 2013; pp. 105–112.
36. Karevan, Z.; Suykens, J.A. Transductive LSTM for time-series prediction: An application to weather forecasting. *Neural Netw.* **2020**, *125*, 1–9. [CrossRef] [PubMed]
37. Zhang, N.; Shen, S.-L.; Zhou, A.; Jin, Y.-F. Application of LSTM approach for modelling stress–strain behaviour of soil. *Appl. Soft Comput.* **2021**, *100*, 106959. [CrossRef]
38. Stollenga, M.F.; Byeon, W.; Liwicki, M.; Schmidhuber, J. Parallel multi-dimensional LSTM, with application to fast biomedical volumetric image segmentation. *Adv. Neural Inf. Process. Syst.* **2015**, 28.
39. Pratap, V.; Hannun, A.; Xu, Q.; Cai, J.; Kahn, J.; Synnaeve, G.; Liptchinsky, V.; Collobert, R. Wav2letter++: A fast open-source speech recognition system. In Proceedings of the ICASSP 2019-2019 IEEE International Conference on Acoustics, Speech and Signal Processing (ICASSP), Brighton, UK, 12–17 May 2019; pp. 6460–6464.
40. Shewalkar, A.; Nyavanandi, D.; Ludwig, S.A. Performance evaluation of deep neural networks applied to speech recognition: RNN, LSTM and GRU. *J. Artif. Intell. Soft Comput. Res.* **2019**, *9*, 235–245. [CrossRef]
41. Oruh, J.; Viriri, S.; Adegun, A. Long short-term memory recurrent neural network for automatic speech recognition. *IEEE Access* **2022**, *10*, 30069–30079. [CrossRef]
42. Gers, F.A.; Pérez-Ortiz, J.A.; Eck, D.; Schmidhuber, J. Learning context sensitive languages with LSTM trained with Kalman filters. In Proceedings of the International Conference on Artificial Neural Networks, Madrid, Spain, 28–30 August 2002; pp. 655–660.
43. Yang, Y.; Xiong, Q.; Wu, C.; Zou, Q.; Yu, Y.; Yi, H.; Gao, M. A study on water quality prediction by a hybrid CNN-LSTM model with attention mechanism. *Environ. Sci. Pollut. Res.* **2021**, *28*, 55129–55139. [CrossRef] [PubMed]
44. Hu, Z.; Zhang, Y.; Zhao, Y.; Xie, M.; Zhong, J.; Tu, Z.; Liu, J. A water quality prediction method based on the deep LSTM network considering correlation in smart mariculture. *Sensors* **2019**, *19*, 1420. [CrossRef] [PubMed]
45. Wang, Y.; Zhou, J.; Chen, K.; Wang, Y.; Liu, L. Water quality prediction method based on LSTM neural network. In Proceedings of the 2017 12th International Conference on Intelligent Systems and Knowledge Engineering (ISKE), Nanjing, China, 24–26 November 2017; pp. 1–5.
46. Zhang, L.; Jiang, Z.; He, S.; Duan, J.; Wang, P.; Zhou, T. Study on water quality prediction of urban reservoir by coupled CEEMDAN decomposition and LSTM neural network model. *Water Resour. Manag.* **2022**, *36*, 3715–3735. [CrossRef]
47. Zhou, J.; Wang, Y.; Xiao, F.; Wang, Y.; Sun, L. Water quality prediction method based on IGRA and LSTM. *Water* **2018**, *10*, 1148. [CrossRef]
48. Zang, C.; Huang, S.; Wu, M.; Du, S.; Scholz, M.; Gao, F.; Lin, C.; Guo, Y.; Dong, Y. Comparison of relationships between pH, dissolved oxygen and chlorophyll a for aquaculture and non-aquaculture waters. *Water Air Soil Pollut.* **2011**, *219*, 157–174. [CrossRef]
49. Lee, J.-H.; Oh, H.-M.; Maeng, J.-S. Water Quality and Phytoplankton Standing Crops in the Daechung Reservoir. *Korean J. Env. Biol.* **2000**, *18*, 355–365.
50. Gwak, N.-T.; Ahn, T.-Y. Eutrophication and Its Countermeasure. *Korean J. Microbiol.* **1997**, *33*, 72–77.
51. Choi, I.-W.; Kim, J.-H.; Im, J.-K.; Park, T.-J.; Kim, S.-Y.; Son, D.-H.; Huh, I.-A.; Rhew, D.-H.; Yu, S.-J. Application of TOC Standards for Managing Refractory Organic Compounds in Industrial Wastewater. *J. Korean Soc. Water Environ.* **2015**, *31*, 29–34. [CrossRef]

52. Virro, H.; Amatulli, G.; Kmoch, A.; Shen, L.; Uuemaa, E. GRQA: Global river water quality archive. *Earth Syst. Sci. Data* **2021**, *13*, 5483–5507. [CrossRef]
53. Nie, Y.; Zhang, R.; Li, S.; Xia, W.; Ma, J. Removal of Microcystis aeruginosa and its extracellular organic matters by using covalently bonded coagulant: An alternative choice in enhanced coagulation for algae-polluted water treatment. *J. Clean. Prod.* **2023**, *419*, 138337. [CrossRef]
54. Abd El-Hack, M.E.; El-Saadony, M.T.; Elbestawy, A.R.; Ellakany, H.F.; Abaza, S.S.; Geneedy, A.M.; Salem, H.M.; Taha, A.E.; Swelum, A.A.; Omer, F.A. Undesirable odour substances (geosmin and 2-methylisoborneol) in water environment: Sources, impacts and removal strategies. *Mar. Pollut. Bull.* **2022**, *178*, 113579. [CrossRef] [PubMed]
55. Okoro, B.U.; Sharifi, S.; Jesson, M.A.; Bridgeman, J. Natural organic matter (NOM) and turbidity removal by plant-based coagulants: A review. *J. Environ. Chem. Eng.* **2021**, *9*, 106588. [CrossRef]
56. Ramli, S.F.; Aziz, H.A. Potential use of tin tetrachloride and polyacrylamide as a coagulant-coagulant aid in the treatment of highly coloured and turbid matured landfill leachate. *Process Saf. Environ. Prot.* **2023**, *170*, 971–982. [CrossRef]
57. Nayak, M.; Rashid, N.; Suh, W.I.; Lee, B.; Chang, Y.K. Performance evaluation of different cationic flocculants through pH modulation for efficient harvesting of *Chlorella* sp. *HS2 and their impact on water reusability. Renew. Energy* **2019**, *136*, 819–827.
58. Lin, Z.; Zhang, C.; Sun, C.; Lu, W.; Quan, B.; Su, P.; Li, X.; Zhang, T.; Guo, J.; Li, W. Treatment of high turbidity mine drainage with iron-based hybrid flocculants: Synthesis process and mechanism, and its interfacial flocculation mechanism. *Sep. Purif. Technol.* **2023**, *327*, 124870. [CrossRef]
59. Jung, Y.-R.; Liu, H.; Kim, Y.-K.; Ye, L.; Chung, S.-W. Effect of Selective Withdrawal on the Control of Turbidity Flow and Its Water Quality Impact in Daecheong Reservoir. *J. Korea Water Resour. Assoc.* **2007**, *40*, 601–615. [CrossRef]
60. Araújo, F.G.; Costa de Azevedo, M.C.; Lima Ferreira, M.d.N. Seasonal changes and spatial variation in the water quality of a eutrophic tropical reservoir determined by the inflowing river. *Lake Reserv. Manag.* **2011**, *27*, 343–354. [CrossRef]
61. Abd Nasier, M.; Abdulrazzaq, K.A. Conventional water treatment plant, principles, and important factors influence on the efficiency. *Des. Eng.* **2021**, 16009–16027.

Disclaimer/Publisher's Note: The statements, opinions and data contained in all publications are solely those of the individual author(s) and contributor(s) and not of MDPI and/or the editor(s). MDPI and/or the editor(s) disclaim responsibility for any injury to people or property resulting from any ideas, methods, instructions or products referred to in the content.